Journal of Biomechanics 206 (2026) 113522

Contents lists available at ScienceDirect

Journal of Biomechanics

journal homepage: www.elsevier.com/locate/jbiomech

The effect of camera configuration on multi-camera markerless motion capture for biomechanical analysis☆

Rebecca Walker [a], Mark A. Robinson [a], Jereme Outerleys [b,c], Leah McKenzie [a], Sven Janecic [a], Nelly Fragoso Vargas [a], Simon Sumner [a], Nathan Winterbone [a], Yu-Hsien Lee [a], Karl C. Gibbon [a], Richard J. Foster [a,*]

[a] Research Institute for Sport and Exercise Sciences, Liverpool John Moores University, Liverpool, United Kingdom
[b] Mechanical and Materials Engineering, Queen's University, Kingston, Ontario, Canada
[c] Theia Markerless Inc., Kingston, Ontario, Canada

ARTICLE INFO

Keywords:
Markerless motion capture
Theia3D
Camera configuration

ABSTRACT

Markerless motion capture technology, such as Theia3D, enables human movement data to be collected outside traditional laboratory environments. However, the extent to which changes in camera configuration influence markerless kinematic output remains underreported. This study evaluated the effect of camera configuration on Theia3D-calculated kinematic parameters during walking, running, and jumping. Ten healthy adults completed five trials of walking, running and counter movement jumps in two volume sizes (10 x 8 m and 6 x 4 m). Movements were captured with eighteen Sony-RX0II synchronised video cameras, which were systematically selected to generate three camera configurations (18-cameras, 12-cameras and 6-cameras), then processed in Theia3D (v2024.1.17). Trunk, pelvis, hip, knee, and ankle kinematics were compared across sagittal, frontal, and transverse planes using one-dimensional statistical parametric mapping. Changes in camera configuration produced mean differences of $< 2^\circ$ during walking, $< 4^\circ$ during running, and $< 3^\circ$ during countermovement jumps. Largest differences were shown for all movements between 18 and 12-camera and 12 and 6-camera configurations in the larger (10 x 8 m) volume. Smallest differences were shown between the 18 and 12 camera configurations in the smaller (6 x 4 m) volume during counter movement jumps. This work demonstrated minimal effects of varying camera configurations on Theia3D markerless kinematics during walking, running and jumping. Camera placement was likely an important factor where small differences were identified. Overall, these findings indicate that Theia3D-derived kinematics are minimally affected by changes in camera configuration during walking, running, and jumping, supporting its use in environments where camera number and space may be constrained.

1. Introduction

Human movement analysis is fundamental to both sport and clinical biomechanics, utilising techniques including two-dimensional (2D) video analysis, three-dimensional (3D) marker-based motion capture, inertial measurement units, and accelerometers (Yeadon & Pain, 2023). While infra-red optoelectronic (marker-based) systems remain the gold standard for accurate kinematic data, they are limited by lengthy marker placement time and the need for dedicated capture spaces with controlled environmental conditions (Armand et al., 2024), as well as susceptibility to marker placement error (Fonseca et al., 2022). These factors can reduce participant throughput, limit accessibility and restrict data collection to controlled laboratory environments, where movement may not fully represent applied sport or clinical settings. Markerless motion capture has emerged as a viable alternative, enabling full-body motion tracking without the need for reflective markers and extending motion capture beyond traditional laboratory settings (McGuirk et al., 2022; Needham et al., 2021).

Theia3D (Theia Markerless Inc., Kingston, ON, Canada) is a commercially available, deep learning–based markerless system that has been used to capture walking, running, and sprinting tasks, demonstrating promising joint angle accuracy and inter-session reliability

☆ This article is part of a special issue entitled: 'Biomechanics in AI Age' published in Journal of Biomechanics.

* Corresponding author.
E-mail address: R.J.Foster@ljmu.ac.uk (R.J. Foster).

https://doi.org/10.1016/j.jbiomech.2026.113522
Accepted 12 August 2026
Available online 12 August 2026

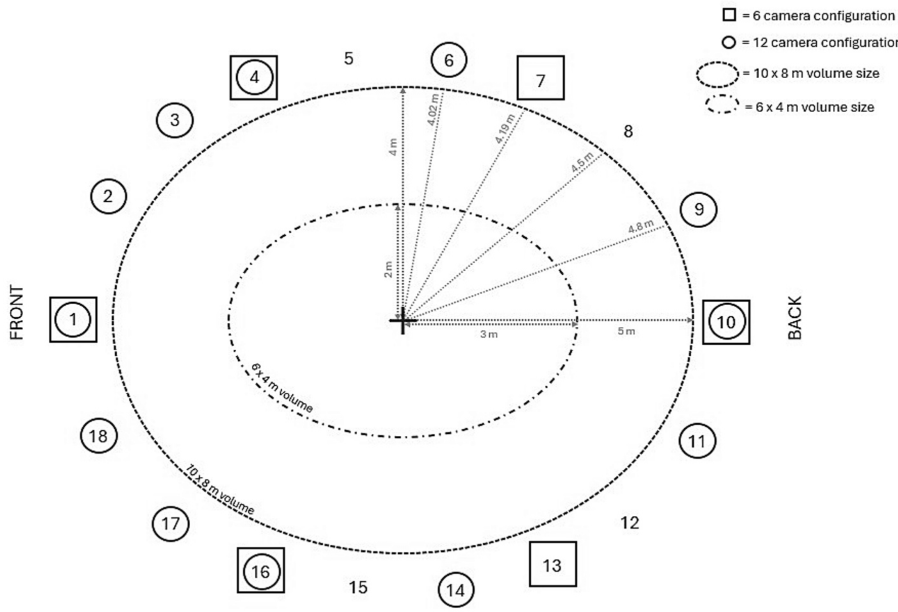

Fig. 1. Schematic of all camera configurations including: Dimensions for 10 x 8 m volume (–‒) and 6 x 4 m volume (–··), with example equal distances between cameras and camera position of all three subsets of camera configurations (6 cameras = □, 12 cameras: ○, and 18 cameras: 1,2,3 etc.).

(Augustine et al., 2025; Kanko, Laende, Selbie, et al., 2021; Kanko et al., 2024; Outerleys et al., 2024; Song et al., 2023). However, accuracy can vary across joints, tasks and individuals (Varcin & Boocock, 2026; Wade et al., 2022), and is influenced by input video characteristics. Camera positioning, number of views, and lighting have been proposed as key factors affecting pose estimation, though their effects remain unclear (Ceriola et al., 2024; Croci et al., 2025; D'Antonio et al., 2021; Nakano et al., 2020).

Existing Theia3D studies have used a variety of camera configurations, including the number of cameras used, spatial arrangement, and capture volume size (Kanko, Laende, Davis, et al., 2021; McGuirk et al., 2022; Oonk et al., 2025; Outerleys et al., 2024; Song et al., 2023). Despite this variability, the influence of camera configuration on kinematic outputs, and the extent to which this influence is driven by algorithmic, environmental, or equipment-related factors is underreported (Varcin & Boocock, 2026). While minimal effects of camera height have been observed (Kwak et al., 2026), the effects of camera number and capture volume size remain unclear. This limits evidence-based setup decisions in applied environments, where users may need to reduce camera numbers, adapt camera placement, or operate within constrained spaces. The aim of this study was to evaluate the effect of camera configuration on Theia3D-calculated kinematic parameters during common movement tasks including walking, running, and jumping. This work aims to inform the use of markerless motion capture systems in research and applied environments where space or camera availability may be limited.

2. Methods

2.1. Participants

Ten healthy adults (7 male, 3 female; age = 31.0 ± 5.1 years, height = 1.8 ± 0.1 m, mass = 73.3 ± 14.3 kg) participated in this study. Participants were excluded if they had any neuromuscular, musculoskeletal, or severe visual impairment, or any cognitive or behavioural condition that prevented them from following instructions. All participants provided written informed consent prior data collection. Ethical approval was granted by the Liverpool John Moores University Research Ethics Committee (Reference: 24/SPS/073).

Participants each completed five trials of walking and running at self-selected speeds from within the volume, and five countermovement jump (CMJ) trials with hands placed on hips (Petrigna et al., 2019) at the centre of the volume. These trials were completed in both the 10 x 8 m and 6 x 4 m volumes, totalling 15 trials per capture volume. Mean walking speed was 1.53 ± 0.12 m/s and mean running speed was 2.94 ± 0.40 m/s. Clothing for each participant is shown in supplementary material 1. All participants wore the same clothing for all conditions.

2.2. Camera configuration

Data were recorded using 18 two-dimensional, colour video cameras (DSC-RX0M2G, Sony Corporation, Japan), capturing at 120 Hz with a shutter speed of 1/1000 s, ISO 12800 and resolution 1920 x 1080 HD (120p 100 M). Cameras were synchronised via Camera Control Boxes (CCB-WD1, Sony Corporation, Japan). Each camera was connected through its multi-terminal interface to a dedicated control box, which were linked to a central Ethernet network switch to enable simultaneous start/stop triggering and unified camera control across devices. Cameras were mounted on tripods at a height of 1.6 m and positioned at equal angular intervals (20° separation) around the centre of an elliptical capture volume.

Two capture volumes were assessed;10 x 8 m and 6 x 4 m. Data were collected using the full 18-camera configuration, with reduced camera configurations (12 and 6 cameras) generated during post-processing by systematically selecting subsets of videos from the full dataset. Camera positions for each configuration are illustrated in Fig. 1, with representative views shown in Fig. 2.

2.3. Camera calibration

Camera calibration was performed using the standard chessboard calibration procedure described in the manufacturer documentation (Theia3D, 2025) with a 7x4 internal corner grid and 100 mm square size. A calibration trial was recorded for each capture volume (10 x 8 m and 6 x 4 m) using all 18 cameras to determine intrinsic and extrinsic parameters within a common coordinate system. Calibration was not repeated before each participant because camera positions remained fixed within each volume condition.

For reduced camera configurations (12 and 6 cameras), the 18-camera calibration files for each volume were duplicated, then video

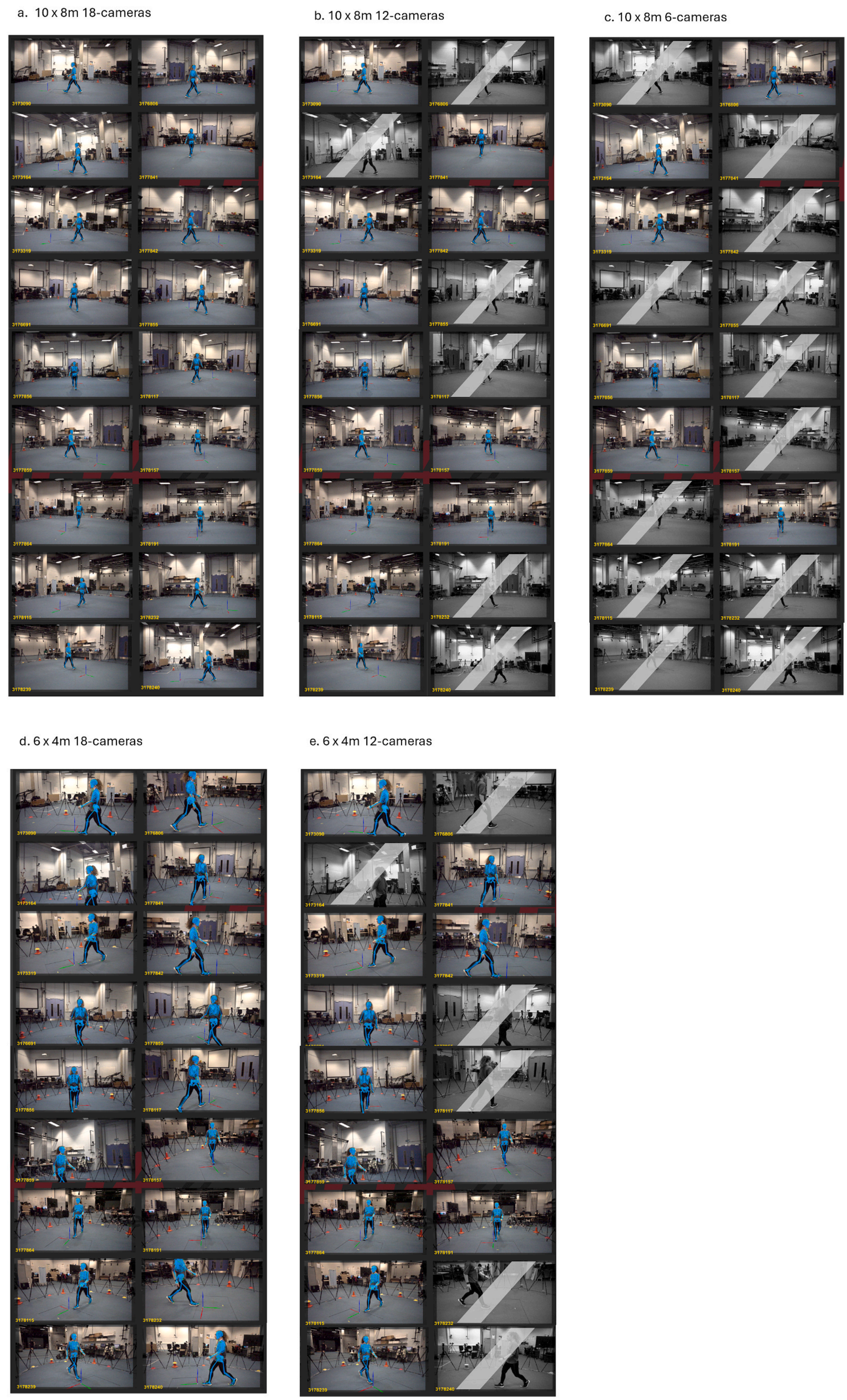

Fig. 2. Camera views for each configuration: a. 10 x 8 m: 18 cameras, b. 10 x 8 m: 12 cameras, c. 10 x 8 m: 6 cameras, d. 6 x 4 m: 18 cameras, e. 6 x 4 m: 12 cameras. Skeletal view shows cameras selected for analysis, grey views with strike through (\) show cameras removed from analysis.

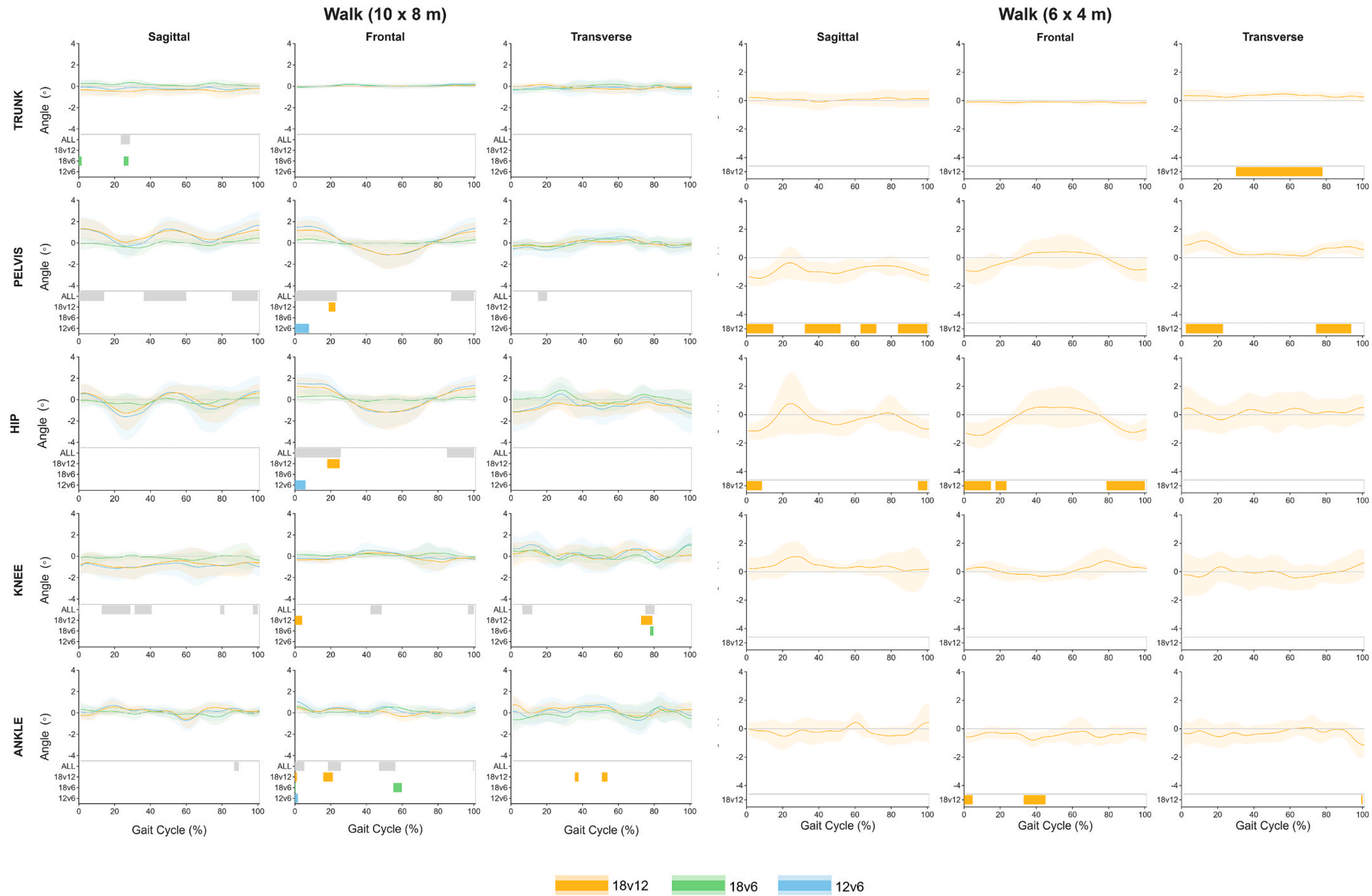

Fig. 3. Joint angle mean differences ± 1SD for walking for the 10 x 8 m volume (left) and 6 x 4 m volume (right). Horizontal bars represent phases of the gait cycle where 1D-SPM identified significant differences between camera configurations. For the 10 x 8 m volume, grey bars represent significant main effects from the 1D-SPM ANOVA and coloured bars represent significant post hoc pairwise comparisons. For the 6 x 4 m volume, coloured bars represent significant paired comparisons between 18 and 12 cameras.

datasets removed to include only the cameras used in the respective configuration. This ensured that any differences between configurations were not due to differences in calibration residuals. Additional calibration trials were recorded with 12 cameras and 6 cameras in both volumes for comparison, with calibration residuals reported in supplementary material 2.

2.4. Data processing

Video images were processed using Theia 3D (v2024.1.17, Theia Markerless Inc., Kingston, ON, Canada), using a full-body model allowing six degrees of freedom at the pelvis and trunk and three degrees of freedom at the ankle, knee and hip. Data from all camera configurations were exported into Visual 3D (v2024.07.2, C-Motion, Canada) for analysis.

For walking and running, the gait cycle (right heel strike to right heel strike) closest to the centre of the capture volume was used for analysis. For walking, this was defined by the point of maximum anterior separation between the heel and pelvis (Zeni et al., 2008), for running, this was determined by the local minima of the vertical velocity of the centre of mass. Countermovement jumps were defined by initiation and termination of vertical centre of mass velocity.

Joint angles at the ankle, knee, hip, pelvis, and trunk were calculated from the 4x4 rotation matrices generated by Theia3D. Kinematics were analysed in the sagittal, frontal and transverse planes. Joint angle data were then filtered using a 6 Hz low-pass Butterworth filter to reduce high-frequency noise and non-physical signal components. This cut-off was consistent with previous markerless motion capture work involving comparable movement tasks and was applied to all configurations, capture volumes, participants, and tasks to ensure that between-configuration differences were not influenced by condition-specific filtering choices. Walking and running trials were time-normalised as a percentage from the start to end of the gait cycle, CMJ trials were time-normalised as a percentage from the initiation of the CMJ to return to typical standing position. Mean joint angles were calculated for each participant for the entire movement then exported to Microsoft Excel (Microsoft 365, Microsoft Corporation). Any trials that were not fully tracked for all joints were removed from analysis, supplementary material 3 shows the distribution of trials removed for all conditions.

2.5. Statistical analysis

One-dimensional statistical parametric mapping (1D-SPM) was used to assess differences between camera configurations across the time-normalised movement cycles (Pataky, 2010). Within the 1D-SPM framework, a one-way repeated-measures analysis of variance (ANOVA) was used for the 10 x 8 m volume to assess for differences between 18, 12 and 6 cameras, followed by post-hoc t-tests. A paired *t*-test was used for the 6 x 4 m volume to assess for differences between 18 and 12 cameras. A two-way ANOVA was not possible since the 6 x 4 m, 6-camera condition was excluded due to an inability to track all segments for some movements caused by restricted camera views. For example, loss of trunk segment tracking during the highest point of a CMJ (supplementary material 3). A statistically significant difference was determined if the SPM{t} curve exceeded the critical threshold with alpha at 0.05. Pairwise camera-configuration comparisons are reported

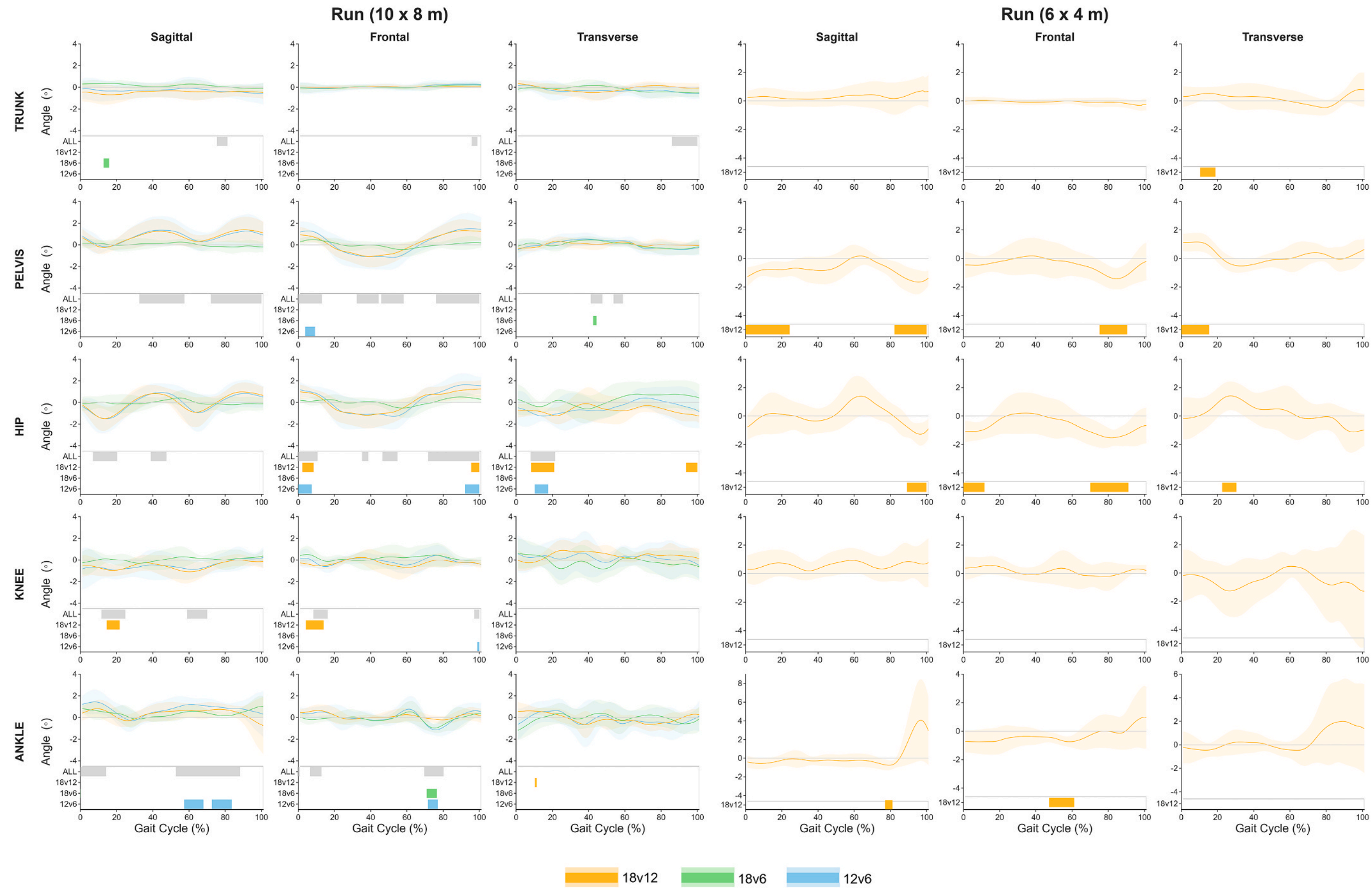

Fig. 4. Joint angle mean differences ± 1SD for running for the 10 x 8 m volume (left) and 6 x 4 m volume (right). Horizontal bars represent phases of the gait cycle where 1D-SPM identified significant differences between camera configurations. For the 10 x 8 m volume, grey bars represent significant main effects from the 1D-SPM ANOVA and coloured bars represent significant post hoc pairwise comparisons. For the 6 x 4 m volume, coloured bars represent significant paired comparisons between 18 and 12 cameras.

as “18v12”, “18v6”, and “12v6”, representing 18 versus 12 cameras, 18 versus 6 cameras, and 12 versus 6 cameras, respectively.

3. Results

Significant differences were observed for walking, running and CMJ in both volume sizes ($P < 0.05$). Mean joint angle differences across all conditions and planes of motion for walking remained < 1.7°, for running < 4.1° and for CMJ < 2.6°. Post-hoc comparison revealed that 18v12 and 12v6 camera configurations accounted for the largest differences in the 10 x 8 m volume for all movements. The smallest differences were shown for CMJ in the 6 x 4 m volume size, for 18v12 camera configurations.

Results for each movement are summarised below including significant differences. In some cases, significant ANOVA results were not supported by post-hoc comparisons. Full 1D-SPM outputs are included in Supplementary Material 4, and joint angle data for each movement are included in Supplementary Material 5.

3.1. 10 x 8 m volume (18 v 12 v 6 cameras)

During walking, the largest mean differences were shown at the pelvis for 18v12 and 12v6 configurations (frontal ≤ 1.6°, sagittal ≤ 1.7°) and smallest at the trunk (all configurations, all planes, ≤0.5°) (Fig. 3). For running, the largest differences occurred for 18v12 and 12v6 camera configurations at the hip (all planes, ≤1.7°), and pelvis (sagittal ≤ 1.4°, frontal ≤ 1.5°), with smallest differences at the trunk (all configurations, all planes, ≤0.7°) (Fig. 4). CMJ results showed largest significant mean differences between 12v6 configurations at the knee (transverse ≤ 2.3°) and ankle (transverse ≤ 2.6°), with mean differences < 2.1° for all other joints and planes (Fig. 5).

3.2. 6 x 4 m volume (18 v 12 cameras)

For walking, the largest differences were observed at the pelvis (sagittal ≤ 1.5°, transverse ≤ 1.2°), and hip (sagittal ≤ 1.2°, frontal ≤ 1.5°), with smallest differences at the trunk (sagittal ≤ 0.3°, frontal ≤ 0.2°) (Fig. 3). Running showed the largest mean differences at the ankle in the last 25% of the gait cycle (all planes, ≤4.1°), all other mean differences remained < 1.7° (Fig. 4). CMJ results showed little significance, with all mean differences < 1.3° (Fig. 5).

4. Discussion

Markerless-derived walking, running, and CMJ kinematics were generally consistent following reductions in camera number within sufficiently large capture volumes. In the 10 x 8 m volume, 18-, 12-, and 6-camera configurations produced mean differences of < 2° during walking, < 4° during running, < 3° during CMJ. In the 6 x 4 m volume, 18- and 12-camera configurations produced comparable outputs; however, the 6-camera configuration resulted in incomplete tracking and was not viable without repositioning. These results indicate that capture volume constraints and camera geometry, rather than camera number alone, influence the magnitude of differences in markerless kinematic outputs.

The differences in markerless kinematics due to camera

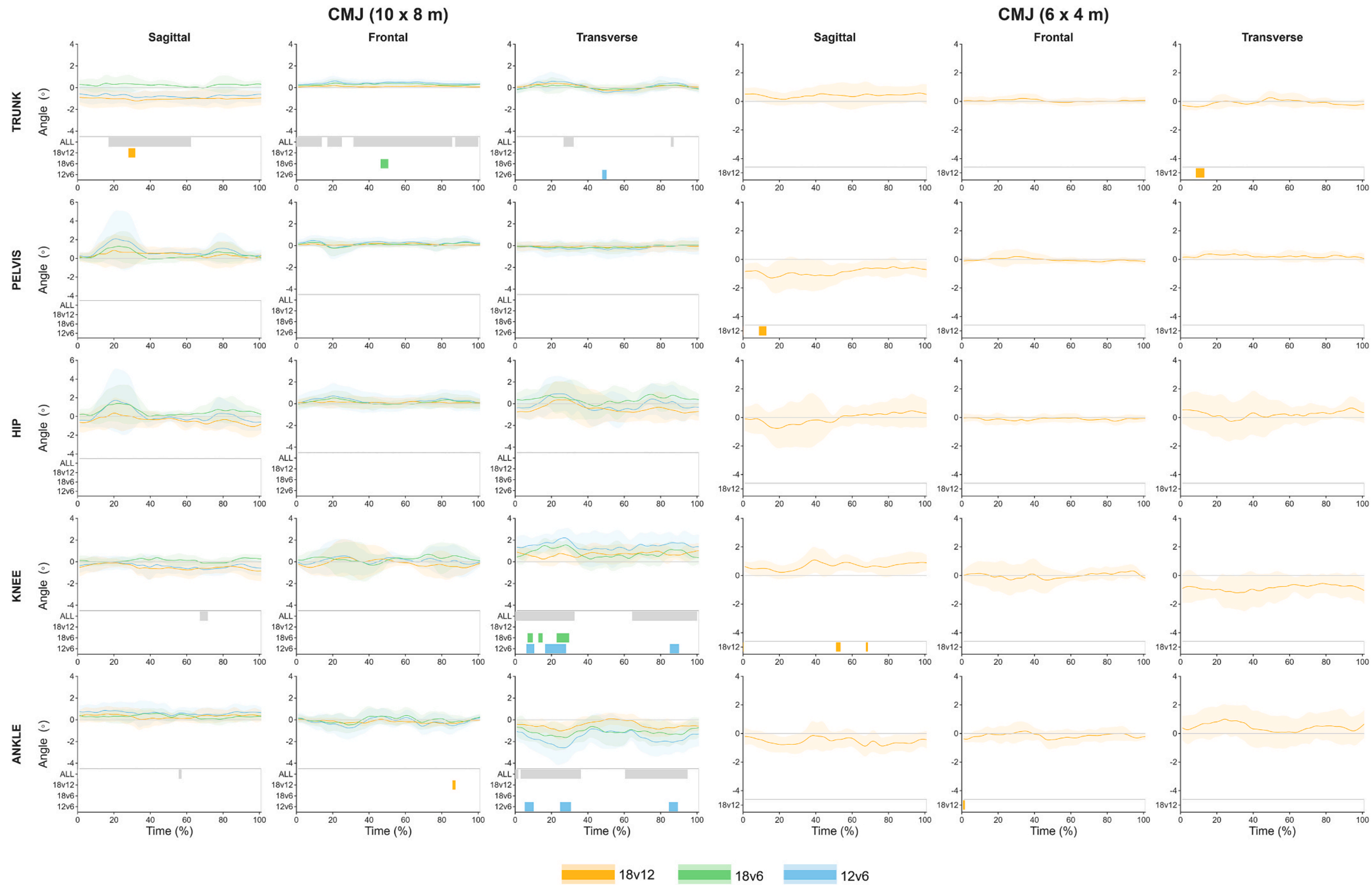

Fig. 5. Joint angle mean differences ± 1SD for CMJ for the 10 x 8 m volume (left) and 6 x 4 m volume (right). Horizontal bars represent phases of the gait cycle where 1D-SPM identified significant differences between camera configurations. For the 10 x 8 m volume, grey bars represent significant main effects from the 1D-SPM ANOVA and coloured bars represent significant post hoc pairwise comparisons. For the 6 x 4 m volume, coloured bars represent significant paired comparisons between 18 and 12 cameras.

configuration in the present study align with recent Theia3D findings reported across variations in camera height (Kwak et al., 2026). Using Theia3D during jumping tasks, that study reported only small significant differences in joint kinematics despite a 1.6 m difference in vertical camera height. Although the largest differences in that study were observed at the hip, whereas the current study showed greater effects at the knee and trunk, this likely reflects differences in camera positioning between the two study designs. More broadly, the between-configuration differences observed here were comparable to, or smaller than, those reported in other Theia3D studies examining methodological factors such as running speed (Walker et al., 2025), clothing condition (Augustine et al., 2025; Keller et al., 2022), and markerless–marker-based comparisons (Kanko et al., 2024; Kearney et al., 2025). This suggests that camera configuration is a relatively modest source of kinematic variation compared with other recognised influences on Theia3D-derived outputs. Importantly, the magnitude of these differences is unlikely to meaningfully affect most applied interpretations.

Differences between camera configurations may have been influenced more by camera geometry than by camera number alone. In the 12-camera configuration, the relative distribution of camera perspectives differed from the evenly spaced 18-camera and 6-camera configurations, changing the angular diversity of views contributing to 3D reconstruction. Camera positions were selected to prioritise front-facing views with greatest likelihood of feature detection, whilst maintaining symmetry and ability to collect a calibration in applied settings. The difference in distribution of views likely contributed to the larger between-condition differences observed in the larger volume. In contrast, CMJ performed centrally within the volume produced minimal differences between the 18- and 12-camera conditions, whereas running near volume boundaries resulted in tracking failures when camera coverage was insufficient. These findings indicate that consistent multi-angle segment visibility as defined by camera placement, rather than camera count alone, underpins stable markerless kinematic outputs. This interpretation is supported by previous work reporting that Theia3D-derived walking and running kinematics were affected by camera position, likely due to joint or segment occlusion and reduced landmark visibility (Thomas et al., 2026).

4.1. Limitations and future work

As no marker-based reference was included our findings indicate configuration-related differences between camera setups rather than the absolute accuracy of each camera configuration. A 6 Hz filtering cut-off was applied across walking, running, and countermovement jumping, which may have attenuated higher-frequency components during the more dynamic tasks, but is expected to influence absolute kinematic magnitudes rather than relative differences between configurations. A single calibration was applied across all camera configurations to isolate the effect of camera number. This method ensured that all differences reflected changes in configuration rather than recalibration effects, however, also reflects results generated from an ideal calibration. When independent calibrations were additionally collected in this work and processed in configurations with fewer cameras, residual error was slightly increased (supplementary material 2), which may be the case in applied settings. Moreover, the 6-camera configuration in the 6 x 4 m volume was excluded due to restricted camera views causing an inability to track all segments for all movements (supplementary material 3), indicating that substantial reductions in camera number without repositioning may compromise segment visibility. The retained camera positions were based on the 18-camera setup, but alternative positioning strategies may improve performance under constrained conditions.

Future work should examine optimised camera placement strategies for restricted environments and directly compare capture volume sizes using configuration-specific calibrations. Investigation across additional sport-specific tasks and participant populations would further clarify the practical limits of markerless motion capture.

5. Conclusion

Theia3D-derived kinematics during walking, running, and countermovement jumping were generally consistent across 18-, 12-, and 6-camera configurations in the 10 x 8 m capture volume. In the smaller 6 x 4 m volume, 18- and 12-camera configurations produced comparable outputs, but the 6-camera configuration was not viable without repositioning due to incomplete segment tracking. These findings indicate that camera number should not be considered in isolation, as capture volume and camera geometry also influence markerless kinematic outputs. When sufficient segment visibility is possible, reduced camera configurations may provide feasible kinematic data for applied environments where space or camera availability is constrained.

CRediT authorship contribution statement

Rebecca Walker: Writing – review & editing, Writing – original draft, Visualization, Validation, Supervision, Software, Resources, Project administration, Methodology, Investigation, Formal analysis, Data curation, Conceptualization. **Mark A. Robinson:** Writing – review & editing, Visualization, Validation, Software, Resources, Methodology, Formal analysis, Data curation, Conceptualization. **Jereme Outerleys:** Writing – review & editing, Validation, Supervision, Conceptualization. **Leah McKenzie:** Writing – review & editing, Validation, Resources, Investigation. **Sven Janecic:** Writing – review & editing, Validation, Resources, Investigation. **Nelly Fragoso Vargas:** Writing – review & editing, Validation, Resources, Investigation. **Simon Sumner:** Writing – review & editing, Validation, Resources, Investigation. **Nathan Winterbone:** . **Yu-Hsien Lee:** Writing – review & editing, Validation, Resources, Investigation. **Karl C. Gibbon:** Writing – review & editing, Writing – original draft, Validation, Supervision, Software, Resources, Methodology, Investigation, Funding acquisition, Data curation, Conceptualization. **Richard J. Foster:** Writing – review & editing, Writing – original draft, Validation, Supervision, Software, Resources, Project administration, Methodology, Investigation, Funding acquisition, Data curation, Conceptualization.

Declaration of competing interest

The authors declare the following financial interests/personal relationships which may be considered as potential competing interests: RW, LM, SJ, NF, SS, NW, YL, KCG and RJF are currently funded by Theia Markerless Inc. for a separate project based at Liverpool John Moores University. This project was not funded by Theia Markerless Inc. JBO is employed by Theia Markerless Inc. No other personnel or resources from Theia Markerless Inc. were involved in the generation or interpretation of these data or manuscript. No other authors have conflicts to disclose.

Appendix A. Supplementary data

Supplementary data to this article can be found online at https://doi.org/10.1016/j.jbiomech.2026.113522.

References

Armand, S., Sawacha, Z., Goudriaan, M., Horsak, B., van der Krogt;, M., Huenaerts, C., Daly, C., Kranzl, A., Boehm, H., Petrarca, M., Guiotto, A., Merlo, A., Spolaor, F., Campanini, I., Cosma, M., Hallemans, A., Horemans, H., Gasq, D., Moissenet, F., Sangeux, M., 2024. Current practices in clinical gait analysis in Europe: a comprehensive survey-based study from the European society for movement analysis in adults and children (ESMAC) standard initiative. Gait Posture 111, 65–74. https://doi.org/10.1016/j.gaitpost.2024.04.014.

Augustine, S., Foster, R., Barton, G., Lake, M.J., Sharir, R., Robinson, M.A., 2025. The inter-trial and inter-session reliability of Theia3D-derived markerless gait analysis in tight versus loose clothing. PeerJ 13, e18613. https://doi.org/10.7717/peerj.18613.

Ceriola, L., Taborri, J., Donati, M., Rossi, S., Patanè, F., Mileti, I., 2024. Comparative analysis of markerless motion capture systems for measuring human kinematics. IEEE Sens. J. 24 (17), 28135–28144. https://doi.org/10.1109/JSEN.2024.3431873.

Croci, E., Künzel, C., Gehring, D., Müller, A.M., Mündermann, A., 2025. Comparison of shoulder kinematics between Theia 3D markerless motion capture and marker-based motion capture during full arm ranges of motion. J. Biomech. 191, 112905. https://doi.org/10.1016/j.jbiomech.2025.112905.

D'Antonio, E., Taborri, J., Mileti, I., Rossi, S., Patané, F., 2021. Validation of a 3D markerless system for gait analysis based on openpose and two RGB webcams. IEEE Sens. J. 21 (15), 17064–17075. https://doi.org/10.1109/JSEN.2021.3081188.

Fonseca, M., Bergere, M., Candido, J., Leboeuf, F., Dumas, R., Armand, S., 2022. The conventional gait model's sensitivity to lower-limb marker placement. Sci. Rep. 12 (1), 14207. https://doi.org/10.1038/s41598-022-18546-5.

Kanko, R.M., Laende, E.K., Davis, E.M., Selbie, W.S., Deluzio, K.J., 2021a. Concurrent assessment of gait kinematics using marker-based and markerless motion capture. J. Biomech. 127, 110665. https://doi.org/10.1016/j.jbiomech.2021.110665.

Kanko, R.M., Laende, E., Selbie, W.S., Deluzio, K.J., 2021b. Inter-session repeatability of markerless motion capture gait kinematics. J. Biomech. 121, 110422. https://doi.org/10.1016/j.jbiomech.2021.110422.

Kanko, R.M., Outerleys, J.B., Laende, E.K., Selbie, W.S., Deluzio, K.J., 2024. Comparison of concurrent and asynchronous running kinematics and kinetics from marker-based and markerless motion capture under varying clothing conditions. J. Appl. Biomech. 40 (2), 129–137. https://doi.org/10.1123/jab.2023-0069.

Kearney, J., Greaves, H., Robinson, M.A., Barton, G.J., O'Brien, T.D., Pinzone, O., Wright, D.M., Gibbon, K., Foster, R.J., 2025. Comparison of Theia3D and the conventional gait model in typically developing children and adults in a clinical gait laboratory. J. Biomech. 193, 112995. https://doi.org/10.1016/j.jbiomech.2025.112995.

Keller, V.T., Outerleys, J.B., Kanko, R.M., Laende, E.K., Deluzio, K.J., 2022. Clothing condition does not affect meaningful clinical interpretation in markerless motion capture. J. Biomech. 141, 111182. https://doi.org/10.1016/j.jbiomech.2022.111182.

Kwak, S.T., Riehm, C.D., Anand, M., Raphael, N., DiCesare, C.A., Schille, A., Hulburt, T. C., Zendler, J.M., Hybart, R.L., Buria, K.N., Trotter, N., Myer, G.D., 2026. Assessing agreement and usability of kinematic measures between markerless and marker-based motion capture systems during jumping activities. J. Biomech. 194, 113065. https://doi.org/10.1016/j.jbiomech.2025.113065.

McGuirk, T.E., Perry, E.S., Sihanath, W.B., Riazati, S., Patten, C., 2022. Feasibility of markerless motion capture for three-dimensional gait assessment in community settings. Front. Hum. Neurosci. 16. https://doi.org/10.3389/fnhum.2022.867485.

Nakano, N., Sakura, T., Ueda, K., Omura, L., Kimura, A., Iino, Y., Fukashiro, S., Yoshioka, S., 2020. Evaluation of 3D markerless motion capture accuracy using openpose with multiple video cameras. Front. Sports Active Living 2. https://doi.org/10.3389/fspor.2020.00050.

Needham, L., Evans, M., Cosker, D.P., Wade, L., McGuigan, P.M., Bilzon, J.L., Colyer, S. L., 2021. The accuracy of several pose estimation methods for 3D joint centre localisation. Sci. Rep. 11 (1), 20673. https://doi.org/10.1038/s41598-021-00212-x.

Oonk, G.A., Kempe, M., Lemmink, K.A.P.M., Buurke, T.J.W., 2025. Examining the concurrent validity of markerless motion capture in dual-athlete team sports movements. J. Sports Sci. 1–12. https://doi.org/10.1080/02640414.2025.2497678.

Outerleys, J., Mihic, A., Keller, V., Laende, E., Deluzio, K., 2024. Markerless motion capture provides repeatable gait outcomes in patients with knee osteoarthritis. J. Biomech. 168, 112115. https://doi.org/10.1016/j.jbiomech.2024.112115.

Pataky, T.C., 2010. Generalized n-dimensional biomechanical field analysis using statistical parametric mapping. J. Biomech. 43 (10), 1976–1982. https://doi.org/10.1016/j.jbiomech.2010.03.008.

Petrigna, L., Karsten, B., Marcolin, G., Paoli, A., D'Antona, G., Palma, A., Bianco, A., 2019. A review of countermovement and squat jump testing methods in the context of public health examination in adolescence: reliability and feasibility of current testing procedures. Front. Physiol. 10, 1384. https://doi.org/10.3389/fphys.2019.01384.

Song, K., Hullfish, T.J., Scattone Silva, R., Silbernagel, K.G., Baxter, J.R., 2023. Markerless motion capture estimates of lower extremity kinematics and kinetics are comparable to marker-based across 8 movements. J. Biomech. 157, 111751. https://doi.org/10.1016/j.jbiomech.2023.111751.

Theia3D. (2025, May 8). Recording Extrinsic Chessboard Calibrations. Recording Extrinsic Chessboard Calibrations | Theia3D Documentation. https://docs.theiamarkerless.com/theia3d-documentation/data-collection/recording-extrinsic-chessboard-calibrations.

Thomas, A., Tucker, C.B., Lunn, D.E., Cooke, M.J., Nicholson, G., Walker, J., 2026. Lights, cameras, action – the influence of lighting and camera position on walking and running kinematic measurements using Theia3D markerless motion capture. J. Biomech. 203, 113343. https://doi.org/10.1016/j.jbiomech.2026.113343.

Varcin, F., Boocock, M.G., 2026. The accuracy, validity and reliability of Theia3D markerless motion capture for studying the biomechanics of human movement: a systematic review. Artif. Intell. Med. 173, 103332. https://doi.org/10.1016/j.artmed.2025.103332.

Wade, L., Needham, L., McGuigan, P., Bilzon, J., 2022. Applications and limitations of current markerless motion capture methods for clinical gait biomechanics. PeerJ 10, e12995. https://doi.org/10.7717/peerj.12995.

Walker, J., Thomas, A., Lunn, D.E., Nicholson, G., Tucker, C.B., 2025. Concurrent validity of Theia3D markerless motion capture for detecting sagittal kinematic differences between gait speeds. J. Sports Sci. 43 (16), 1560–1571. https://doi.org/10.1080/02640414.2025.2513151.

Yeadon, M.R., Pain, M.T.G., 2023. Fifty years of performance-related sports biomechanics research. J. Biomech. 155, 111666. https://doi.org/10.1016/j.jbiomech.2023.111666.

Zeni, J.A., Richards, J.G., Higginson, J.S., 2008. Two simple methods for determining gait events during treadmill and overground walking using kinematic data. Gait Posture 27 (4), 710–714. https://doi.org/10.1016/j.gaitpost.2007.07.007.